

International Conference on Space Optics—ICSO 2022

Dubrovnik, Croatia

3–7 October 2022

Edited by Kyriaki Minoglou, Nikos Karafolas, and Bruno Cugny,



Development of T2SLS LWIR focal plane arrays for the hyperspectral thermal imager (HyTI)



Development of T2SLS LWIR focal plane arrays for the hyperspectral thermal imager (HyTI)

Sarath Gunapala, David Ting, Sir Rafol, Alexander Soibel, Arezou Khoshakhlagh, Sam Keo, Brian Pepper, Anita Fisher, and Cory Hill
Center for Infrared Photodetectors, Jet Propulsion Laboratory, California Institute of Technology
Pasadena, California, USA

Ashok Sood and John Zeller
Magnolia Optical Technologies, Inc, Albany New York 12203, USA

Paul Lucey, Robert Wright, Miguel Nunes, and Luke Flynn
Hawaii'i Institute of Geophysics and Planetology, University of Hawaii'i at Manoa, Honolulu,
Hawaii, USA

Sachidananda Babu and Parminder Ghuman
NASA Earth Science Technology Office
Greenbelt, Maryland, USA

ABSTRACT

In this presentation, we will report our recent efforts in achieving high performance in Antimonides type-II strained layer superlattice (T2SLS) based infrared photodetectors using the barrier infrared detector (BIRD) architecture. The high operating temperature (HOT) BIRD focal plane arrays (FPAs) offer the same high performance, uniformity, operability, manufacturability, and affordability advantages as InSb. However, mid-wavelength infrared (MWIR) HOT-BIRD FPAs can operate at significantly higher temperatures (>150K) than InSb FPAs (typically 80K). Moreover, while InSb has a fixed cutoff wavelength (~5.4 μm), the HOT-BIRD offers a continuous adjustable cutoff wavelength, ranging from ~4 μm to >15 μm , and is therefore also suitable for long wavelength infrared (LWIR) as well. The LWIR detectors based on the BIRD architecture has also demonstrated significant operating temperature advantages over those based on traditional p-n junction designs. Two 6U SmalSat mission HyTI (Hyperspectral Thermal Imager) are based on JPL's T2SLS BIRD FPAs. Based on III-V compound semiconductors, the BIRD FPAs offer a breakthrough solution for the realization of low cost (high yield), high-performance FPAs with excellent uniformity and pixel-to-pixel operability.

Keywords: type-II strained layer superlattice, infrared detector, long-wavelength infrared, quantum efficiency, focal plane arrays

1. INTRODUCTION

Hyperspectral Thermal Imager (HyTI) is designed with the focus on understanding, modeling, mapping, and monitoring the world's agricultural lands, and water resources, as well as for studies pertaining to forest fires, volcanoes, and a number of other applications (e.g., stubble burning in agricultural lands). Climate variability and expanding populations are putting unprecedented pressure on agricultural croplands and their water use, which are vital for ensuring global food and water security in the twenty-first century. Currently, on average worldwide, croplands use 80-90% of all human water consumption. HyTI data and derived information products will be invaluable in advancing our knowledge on multiple fronts in crop type mapping, crop productivity modeling, crop water use assessments, and crop water productivity ("crop per drop") mapping.

Retrievals of land surface temperature (LST) from hyperspectral imagery has been made for over two decades. [1-8] By using one or more of these previously established methods for LST retrieval, we believe accuracies of ≤ 1 K are potentially achievable from HyTI hyperspectral imagery. The primary benefits of demonstrating HyTI's spaceborne hyperspectral TIR imaging capability are:

a. Significantly Reduced Cost: Demonstration of high spatial and spectral resolution TIR imaging capability using a 6U CubeSat platform represents the lowest possible cost for a scientific grade, Earth Observing mission. The low cost of the HyTI LEO mission will also make possible, in the future, high-temporal resolution, global coverage by putting up a constellation of between 25-30 HyTI satellites for well under the budget required for a single, conventional satellite such as LandSat-8.

b. New and Enhanced Science Capability: As mentioned above, hyperspectral TIR imaging with high spatial resolution has thus far not been achieved from space. Using a combination of advanced signal processing and sensor fusion algorithms, not only will we be able to derive very accurate LST values for a wide range of land surfaces (i.e., soil, vegetation, water bodies etc.) but, and for the first time, HyTI data and information products will be "actionable" at the individual farm level due to the high spatial resolution. HyTI data will enable the development of new hyperspectral narrowband thermal indices for monitoring crop stress, crop water productivity (crop per drop), crop water use, irrigated crop type mapping and modeling, and ultimately, overall crop productivity and harvest yield predictions.

2. HYPERSPECTRAL THERMAL IMAGER (HyTI) PROJECT

HyTI is NASA Earth Science Technology Office's In-space Validation of Earth Science Technologies (InVEST) 2018 funded project to space qualify the strained layer superlattice based Barrier Infrared Detector (BIRD) Focal Plane Array [1], Fabry-Perot Interferometer, and Unibap e2160 heterogeneous computer specifically designed for small satellites operation. JPL's Barrier Infrared Detector (BIRD) technology based on III-V compound semiconductors offers a breakthrough solution for the realization of low cost, high-performance FPAs with excellent uniformity and pixel-to-pixel operability. The Unibap e2160 possesses a TRL-9 [9], safety critical, space-proven computer architecture that directly addresses high throughput image data processing applications.

3. LWIR FOCAL PLANE ARRAY DEVELOPMENT

The InAs/InAsSb type-II strained layer superlattice (T2SLS) has emerged as an alternative adjustable bandgap, broad-band III-V IR detector material to the more established InAs/GaSb type-II superlattice (T2SL).

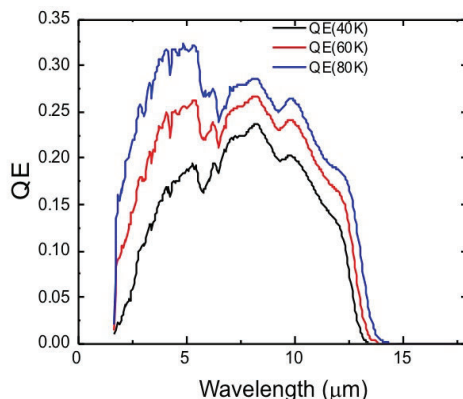


Figure 1. Backside illuminated spectral quantum efficiency (QE) for an LWIR detector measured at temperatures ranging from 40K to 80K.

Recently, there has been growing interest in this material as an infrared detector absorber due to longer MWIR and LWIR minority carrier lifetimes in InAs/InAsSb T2SLS than in InAs/GaSb superlattice T2SL and demonstrated an InAs/InAsSb T2SLS LWIR photodetector based on the nBn device design [7]. The T2SLS material can be grown on InAs or GaSb substrates, GaSb is available in 2”, 3”, 4” and 6” diameters formats. An InAs/InAsSb SLS nBn structure was grown on a 4-inch diameter low Te-doped GaSb (100) substrate in a Veeco Applied-Epi Gen III molecular beam epitaxy chamber equipped with valved cracking sources for the group V Sb₂ and As₂ fluxes. The nBn architecture is used for G-R and surface-leakage dark current suppression. Square mesa photodiodes of area 250μm x 250μm were fabricated along with detector arrays for responsivity and dark current measurements. The devices were not passivated nor treated with anti-reflection coating. Figure 1 shows the spectral quantum efficiency (QE) derived from back-side illuminated (through the GaSb substrate) spectral responsivity measured at temperatures ranging from 40K to 80K; the QE has not been corrected for substrate reflection or transmission. Accordingly, the spectral QE for 40K and 80K was taken at -50mV. The cutoff, taken at the wavelength at which the QE is 50% of that at λ=12.5μm.

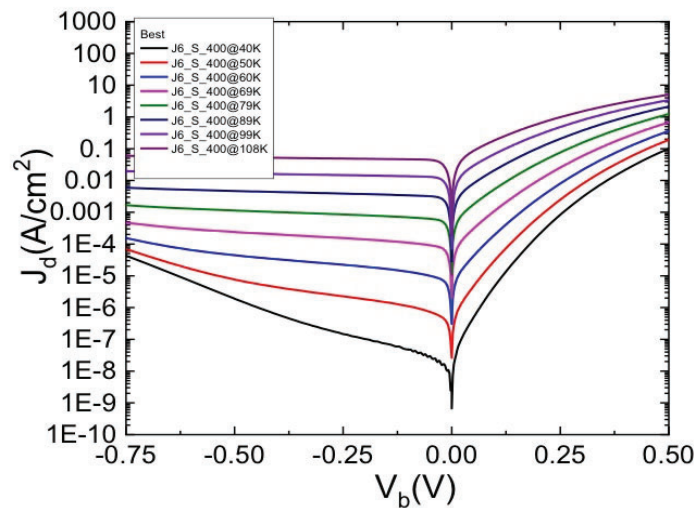


Figure 2 Dark current density (J_d) as a function of applied bias, measured at temperatures ranging from 40K to 108K.

Figure 2 shows the measured dark current density as a function of applied bias for temperatures ranging from 40K to 108K. The -50mV dark current density at 60K is $2.6 \times 10^{-5} \text{ A/cm}^2$. The presence of G-R dark current is apparent from the shapes of the J-V curves in Fig. 2 at temperatures below 60K; tunneling current can also be seen at lower temperatures and high reverse bias.

The detector material was used to fabricate 24μm pitch, 640x512 format arrays and hybridized to the SBF-193 readout integrated circuit (ROIC). The detector mesas are etched to just below the barrier; the pixels are not fully reticulated.

This engineering grade HyTI FPA without anti-reflection coating (ARC), has given 31% quantum efficiency in 8-9.4 μm spectral bands at 68K operating temperature (see Figure 3). Figure 4 shows the quantum efficiency histogram of the FPA. Substrate of the FPA was removed leaving only 30μm. As a result, Fabry Perot oscillations was observed on the quantum efficiency spectrum of the FPA.

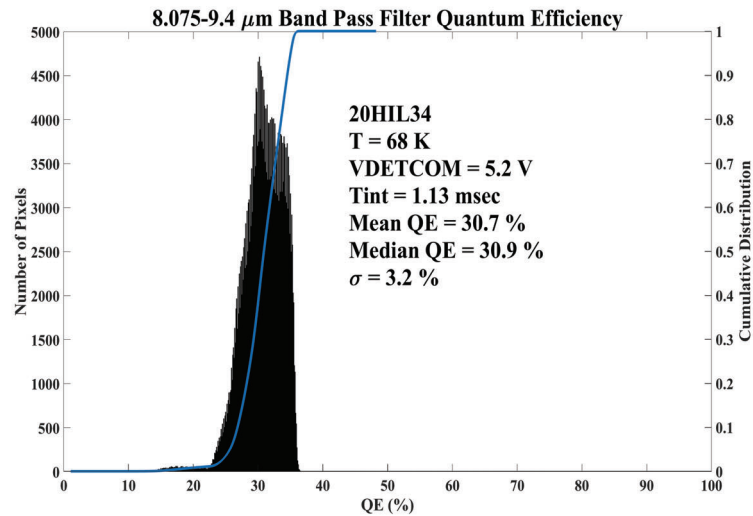


Figure 3 8-9.4 μm filter QE of the LWIR BIRD focal plane array (FPA) without antireflection coating at 68K.

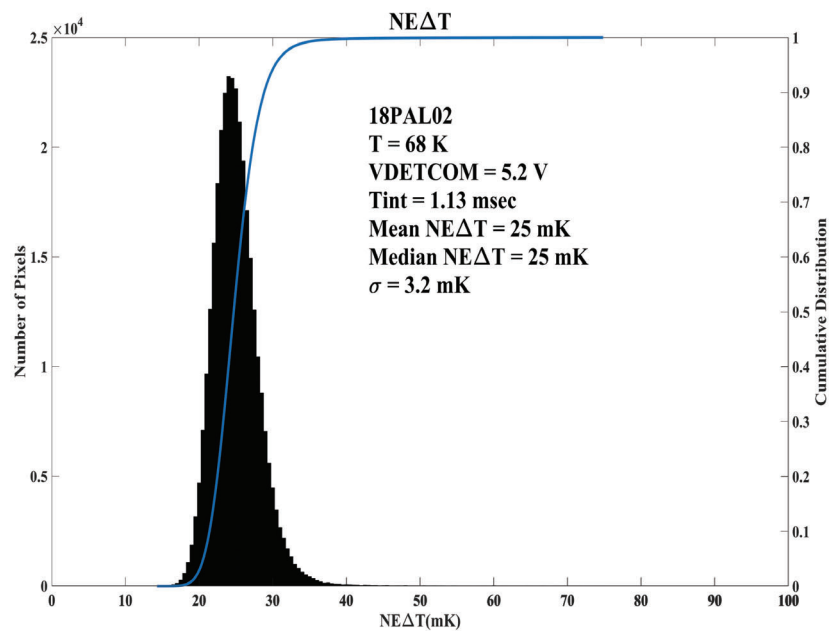


Figure 4 8-9.4 μm broad-bandpass filter QE of the LWIR BIRD focal plane array (FPA) at 62K.

The noise equivalent temperature difference (NE Δ T) provides the thermal sensitivity of an infrared imaging system and it is a very useful diagnostic tool to evaluate the full operational performance available. It is defined as the minimum temperature difference required at the target to produce unity signal-to-noise-ratio. Sequence of consecutive frames is collected for equivalent noise determination as well as other optical properties of FPA. The photo response matrices of FPA is derived at the low and high blackbody temperatures (i.e., 295 K and 305 K), and temporal noise matrix of FPA is estimated at the mid-point temperature by taking 64 frames of data. The temporal NE Δ T of pixels are numerically evaluated from the relations, NE Δ T =

$\sigma_{\text{Temporal}}\Delta T/[\text{Mean}(T_H) - \text{Mean}(T_L)]$. The mean signal $\text{Mean}(T_L)$ and $\text{Mean}(T_H)$ are evaluated at blackbody temperatures of $T_L = 295 \text{ K}$ and $T_H = 305 \text{ K}$. The temporal noise is measured at 300K using 64 frames, and $\Delta T \sim 10 \text{ K}$.

The experimentally measured NE ΔT histograms distributions of 640x512 pixels LWIR BIRD FPA at 62K operating temperature with blackbody temperature of 300 K and f/4 cold stop is shown in the Fig. 4. The experimentally measured NE ΔT of 16.3mK is in fair agreement with the estimated NE ΔT value based on the results of a single element test detector data. This engineering grade FPA was used to build the HyTI engineering model instrument as shown in Figure 5.

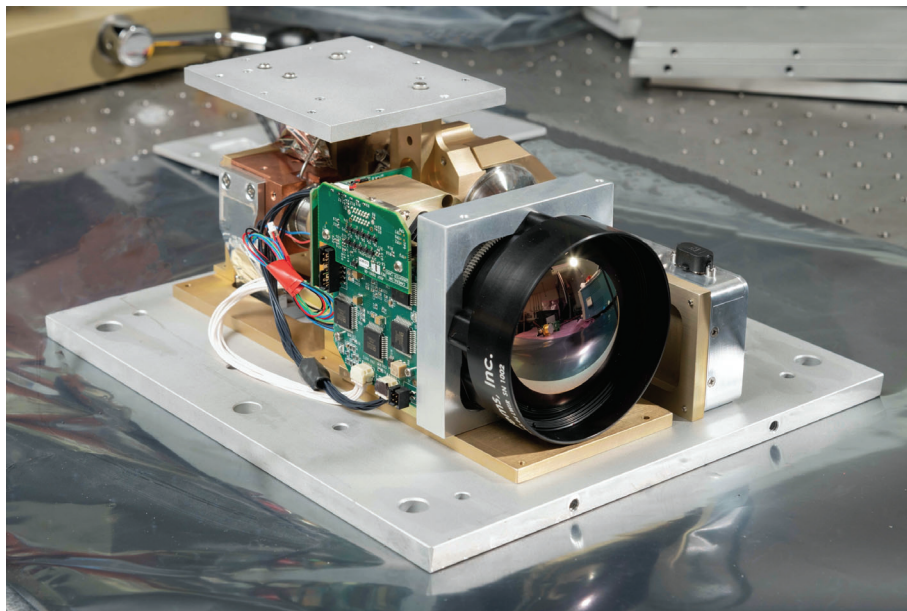


Figure 5. Engineering model of the HyTI Instrument.

4. ANTIREFLECTION COATING

Nearly 35% of the incoming infrared radiation get reflected off due the high refractive index of the GaSb substrate. Broadband antireflection (AR) optical coatings covering the complete infrared spectral band have many potential applications for various observational instruments. AR coatings not only improve the quantum efficiency of the FPA, but it also reduces the backscattered radiation within the instrument. Furthermore, it reduces the Fabry Perot oscillation observed in the engineering grade HyTI FPA. Reduction of Fabry Perot oscillations is very important for the HyTI interferometer which also produce its own signal dependent fringe pattern.

Therefore, we have deposited Magnolia Optical Technologies' nanostructured novel AR coating [10] on to the substrate of the HyTI flight FPAs. This AR coating substantially improved the quantum efficiency (from 31% to 47%) of the FPA, while minimizing reflection losses over a wide range of incidence angles, providing substantial improvements over conventional thin film AR coating technologies as shown of Figure 6.

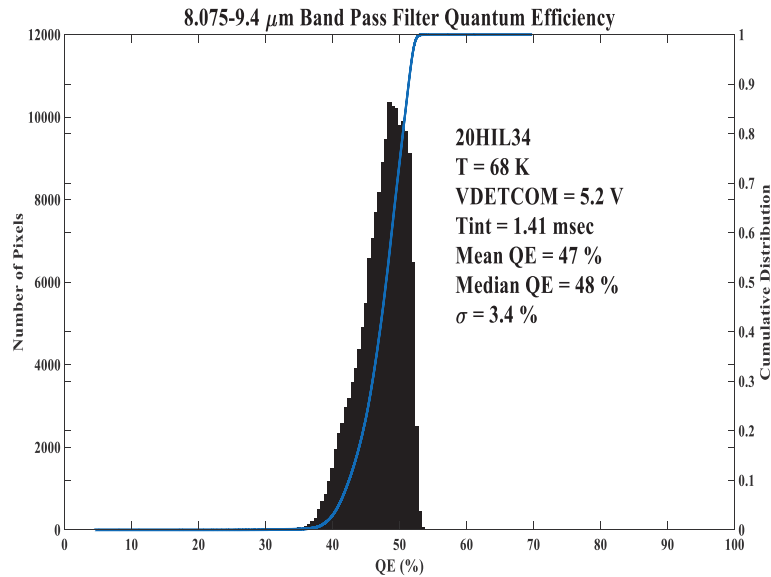


Figure 6. 8-9.4 μm filter QE of the LWIR BIRD focal plane array (FPA) with antireflection coating at 68K.

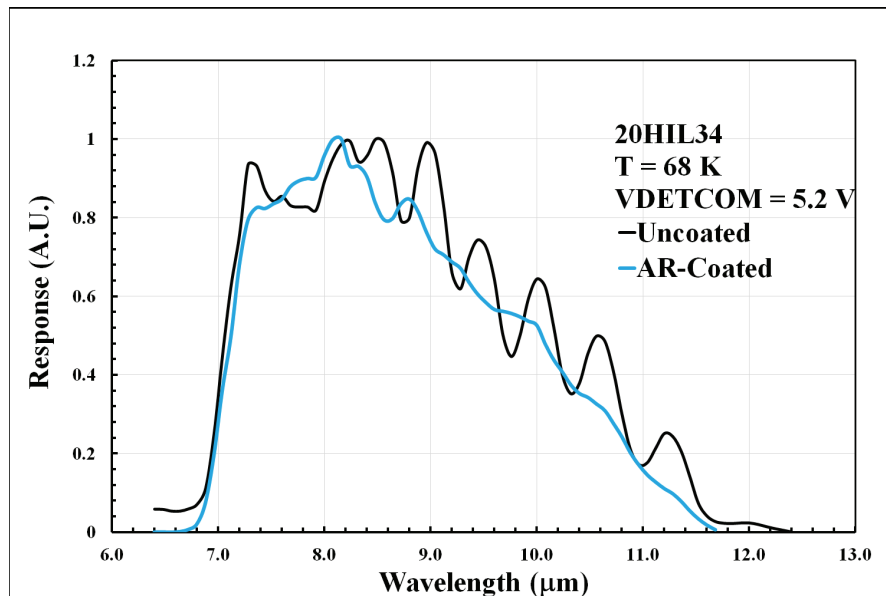


Figure 7. This figure shows the effect of the AR coating in reducing the Fabry Perot oscillations. No reference detector normalization. In this measurement, we were interested in capturing oscillations with respect to wavelength. Band pass filter 6.8 μm to 12.4 μm

Figure 7 shows the effect of the AR coating in reducing the Fabry Perot oscillations. No reference detector normalization. In this measurement, we were interested in capturing oscillations with respect to wavelength. Band pass filter 6.8 μm to 12.4 μm . This flight FPA is being integrated with the HyTI flight instrument during the preparation of this extended manuscript.

5. SUMMARY

HyTI is designed with the focus on understanding, modeling, mapping, and monitoring the world's agricultural lands, and water resources, as well as for studies pertaining to forest fires, volcanoes, and a number of other applications. It is NASA ESTO InVEST 2017 funded project to space qualify the BIRD FPA, Fabry-Perot Interferometer, nanostructured AR coating, and Unibap e2160 heterogeneous computer. HyTI instrument is expected to be launched in the second half of 2022 on a 6U CubeSat platform.

ACKNOWLEDGEMENT

The authors thank the NASA Earth Science Technology Office and Jason Hyon and Eastwood Im of Jet Propulsion Laboratory for encouragement and support. The research described in this paper was carried out at the Jet Propulsion Laboratory, California Institute of Technology, under a contract with the National Aeronautics and Space Administration. © 2022. All rights reserved. Government sponsorship acknowledged.

REFERENCES

1. French, A. N., J. M. Norman, and M. C. Anderson (2003), A simple and fast atmospheric correction for spaceborne remote sensing of surface temperature, *Remote Sens. Environ.*, 87, 326–333.
2. Sobrino, J. A., and Raissouni, N. (2000). Toward remote sensing methods for land cover dynamic monitoring. Application to Morocco. *International Journal of Remote Sensing*, 21, 353–366.
3. Wan, Z.M.; Li, Z.L. A physics-based algorithm for retrieving land-surface emissivity and temperature from eos/modis data. *IEEE Trans. Geosci. Remote Sensing* 1997, 35, 980–996.
4. Masiello, G.; Serio, C.; De Feis, I.; Amoroso, M.; Venafrà, S.; Trigo, I.F.; Watts, P. Kalman filter physical retrieval of surface emissivity and temperature from geostationary infrared radiances. *Atmos. Meas. Tech.* 2013, 6, 3613–3634.
5. Ma, X.L.; Wan, Z.M.; Moeller, C.C.; Menzel, W.P.; Gumley, L.E.; Zhang, Y.L. Retrieval of geophysical parameters from moderate resolution imaging spectroradiometer thermal infrared data: Evaluation of a two-step physical algorithm. *Appl. Opt.* 2000, 39, 3537–3550.
6. Ma, X.L.; Wan, Z.M.; Moeller, C.C.; Menzel, W.P.; Gumley, L.E. Simultaneous retrieval of atmospheric profiles, land-surface temperature, and surface emissivity from moderate-resolution imaging spectroradiometer thermal infrared data: Extension of a two-step physical algorithm. *Appl. Opt.* 2002, 41, 909–924.
7. Zhong, X., X. Huo, C. Ren, J. Labed, and Z.-L. Li, Retrieving land surface temperature from hyperspectral thermal infrared data using a multi-channel method. *Sensors* 2016, 16, 687; doi:10.3390/s16050687.
8. Sobrino, J. A., J. C. Jimenez-Munoz, P. J. Zarco-Tejada, G. Sepulcre-Canto, and E. de Miguel, Land surface temperature derived from airborne hyperspectral scanner thermal infrared data. *Remote Sensing of Environment* 102 (2006) 99–1154.
9. Unibap (<https://unibap.com/>) heterogeneous computers have been successfully flown and operated on Satellogic (<https://www.satellogic.com/>) spacecraft.
10. D. Z. Ting, A. Soibel, A. Khoshakhlagh, S. B. Rafol, S. A. Keo, L. Höglund, A. M. Fisher, E. M. Luong, and S. D. Gunapala, “Mid-wavelength high operating temperature barrier infrared detector and focal plane array”, *Appl. Phys. Lett.* 113 , 021101 (2018). doi: 10.1063/1.5033338

11. David Z. Ting, Alexander Soibel, Arezou Khoshakhlagh, Sam A. Keo, Anita M. Fisher, Sir B. Rafol, Linda Höglund, Cory J. Hill, Brian J. Pepper, and Sarath D. Gunapala, Long wavelength InAs/InAsSb superlattice barrier infrared detectors with p-type absorber quantum efficiency enhancement, *Appl. Phys. Lett.* 118, 133503 (2021); <https://doi.org/10.1063/5.0047937>
12. Ashok K. Sood, Dr. John W Zeller, Adam W Sood, Roger E. Welser, Harry Efstathiadis, Parminder Ghuman, Sachidananda Babu, Sarath Gunapala, Development of UV to IR band nanostructured antireflection coating technology for improved detector and sensor performance, *Proc. SPIE 11723, Image Sensing Technologies: Materials, Devices, Systems, and Applications VIII*, 117230F (21 May 2021); doi: 10.1117/12.2591158